

Dispersion-compensating en/decoder for a time-spreading/wavelength-hopping optical code-division multiplexing (OCDM) system

JILIN ZHENG^{1*}, RONG WANG¹, TAO PU¹, LIN LU¹, TAO FANG¹,
YANG SU¹, LING LI², QIAN YANG³, XIANGFEI CHEN³

¹Photonic Information Technology Lab, Institute of Communication Engineering,
PLA University of Science and Technology, Nanjing 210007, P.R. China

²Engineering Institute of Engineering Corps, PLA University of Science and Technology,
Nanjing 210007, P.R. China

³National Lab of Microstructure, Nanjing University, Nanjing 210093, P.R. China

*Corresponding author: zhengjilinjs@126.com

A novel dispersion-compensating fiber Bragg grating (FBG)-based en/decoder is proposed to compensate both the out-band and in-band dispersion in a time-spreading/wavelength-hopping (TS/WH) optical code-division multiplexing (OCDM) system. The experimental realization of such en/decoders only needs a uniform-pitch phase mask and a sub-micrometer precision moving stage. Such an en/decoder pair with the ability of compensating the dispersion of transmission in 20-km single mode fiber (SMF) is simulated and experimentally fabricated. Both the simulation and experimental results show that the decoded pulse can be recovered without any distortion owing to the elimination of dispersion.

Keywords: optical code-division multiplexing (OCDM), fiber Bragg grating (FBG), dispersion.

1. Introduction

The optical code-division multiplexing (OCDM) is a spectrum-spreading technology in the optical domain, which takes advantage of the extremely wide bandwidth of optical transmission medium to achieve multiplexing and multiple-access. The OCDM is regarded as a very important multiplexing technology due to its attractive abilities, such as all-optical processing, asynchronous transmission, simplified networking and so on [1–7]. On the other hand, as propagating in the dispersive transmission medium, the wide-band OCDM signals will suffer serious distortion, e.g., group delay caused by the wavelength dispersion in the single mode fiber (SMF). Using an extra dispersion-compensating component is a routine solution but not a cost-effective way.

En/decoder within a group delay compensation function is a novel approach to solving the dispersion problem. In the previous research, literature [8] firstly proposed time-spreading/wavelength-hopping (TS/WH) group delay compensating a fiber Bragg grating (FBG) en/decoder, which validated the feasibility of such concepts experimentally. However, such en/decoders need to be improved if applied into practice. First, the FBG fabrication equipment, such as phase masks, is required to vary with the address-code or the amount of dispersion-compensation, which increases the complexity and cost of experimental realization. Second, the in-band dispersion cannot be compensated, which will deteriorate the system performance, especially in the case of longer transmission distance or higher data rate.

In this work, we develop a novel dispersion compensating FBG-based en/decoder. Compared with the previous dispersion compensating en/decoder, our new technology is easier to be experimentally realized, and most importantly, the in-band dispersion can also be compensated. Such advances are expected to make the dispersion compensating en/decoder more practical.

2. Principle

Figure 1 shows the $\tau-\lambda$ (*i.e.*, time-delay versus wavelength) distribution of TS/WH signals evolving at different stages. The address code used here is the prime-hop sequence (P0H2, $p = 5$) used in [8]. It can be seen after propagating in the G.652 fiber that there is not only extra relative group delay among different wavelength-chips, but also extra dispersion inside one chip. As reported in literature [8], the “decoding A” in this figure represents using an out-band dispersion compensating decoder. Such a decoder cannot compensate the in-band dispersion, and the residual dispersion will result in pulse broadening and deteriorate the system performance. However, this paper proposes the “decoding B” technique, which uses a total dispersion (both out-band and in-band) compensating decoder, and can completely compensate all the dispersion.

For the encoded signals, the time delay between one tip pulse (central wavelength λ_1) and another tip pulse (central wavelength λ_i) is defined as ΔT_i^{enc} ($i = 2, 3, \dots, p$, p is the number of wavelengths). When the encoded signals propagate in the SMF with the length of z , an extra time delay $\Delta T_i^{\text{out-disp}}$ ($i = 2, 3, \dots, p$) among tip pulses is added:

$$\Delta T_i^{\text{out-disp}} = Dz(\lambda_i - \lambda_1) \quad (1)$$

where D is the wavelength dispersion coefficient of SMF. On the other hand, every reflective channel of the encoding spectrum occupies a certain bandwidth, which is defined as $\Delta\lambda$ in this paper ($\Delta\lambda < \min(\lambda_i - \lambda_j)$, $i \neq j$). So the in-band dispersion $\Delta T_{i, (\lambda - \lambda_i)}^{\text{in-disp}}$ ($i = 1, 2, \dots, p$) inside one chip is produced:

$$\Delta T_{i, (\lambda - \lambda_i)}^{\text{in-disp}} = Dz(\lambda - \lambda_i), \quad |\lambda - \lambda_i| \leq \frac{\Delta\lambda}{2} \quad (2)$$

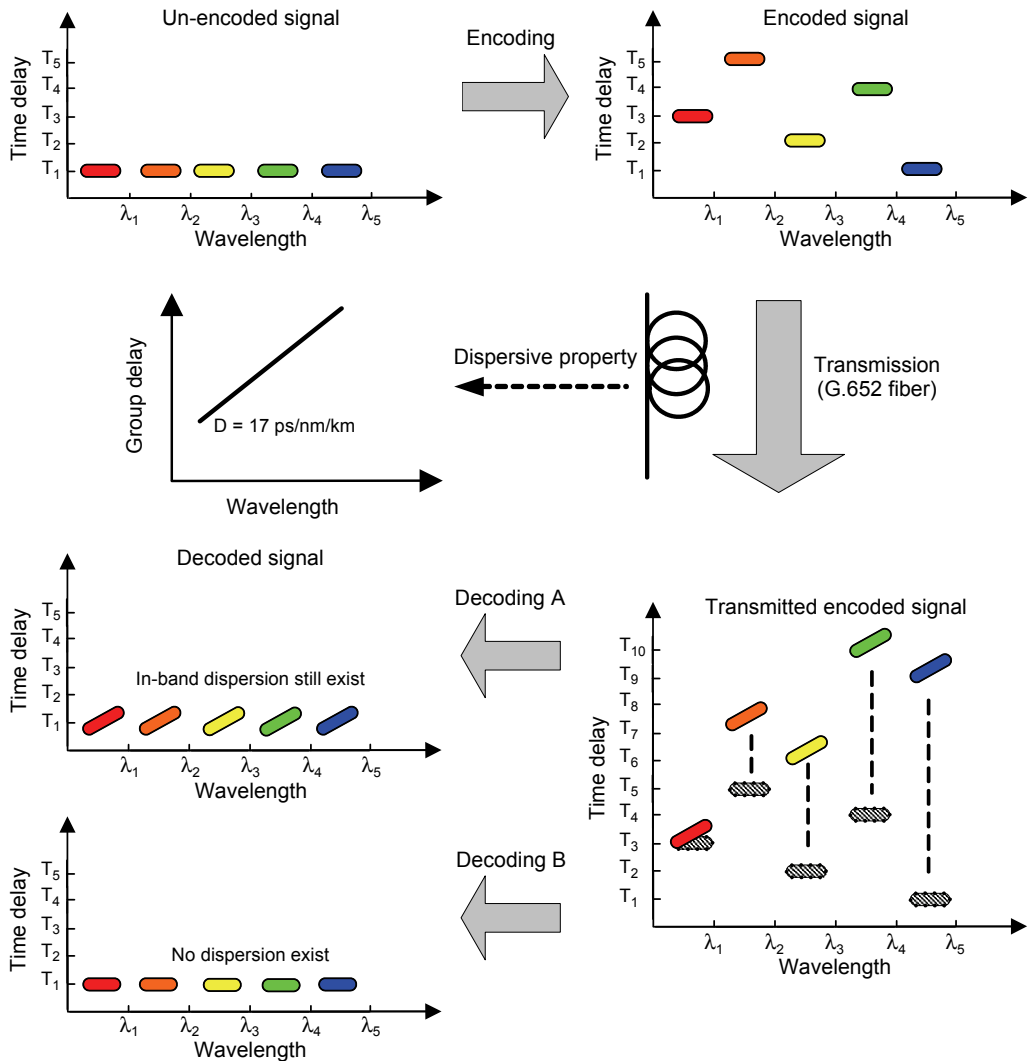


Fig. 1. The τ - λ distribution of TS/WH signals evolving at different stages. Decoding A – using out-band dispersion compensating decoder; decoding B – using total dispersion (both out-band and in-band) compensating decoder.

In order to compensate all the dispersion, the time delay of the decoder ΔT_i^{dec} ($i = 1, 2, \dots, p$) should satisfy the following condition:

$$\Delta T_{i, (\lambda - \lambda_i)}^{\text{dec}} = \begin{cases} -(\Delta T_i^{\text{enc}} + \Delta T_i^{\text{out-disp}} + \Delta T_{i, (\lambda - \lambda_i)}^{\text{in-disp}}) & i \neq 1 \\ -\Delta T_{i, (\lambda - \lambda_i)}^{\text{in-disp}} & i = 1 \end{cases}, \quad |\lambda - \lambda_i| \leq \frac{\Delta \lambda}{2} \quad (3)$$

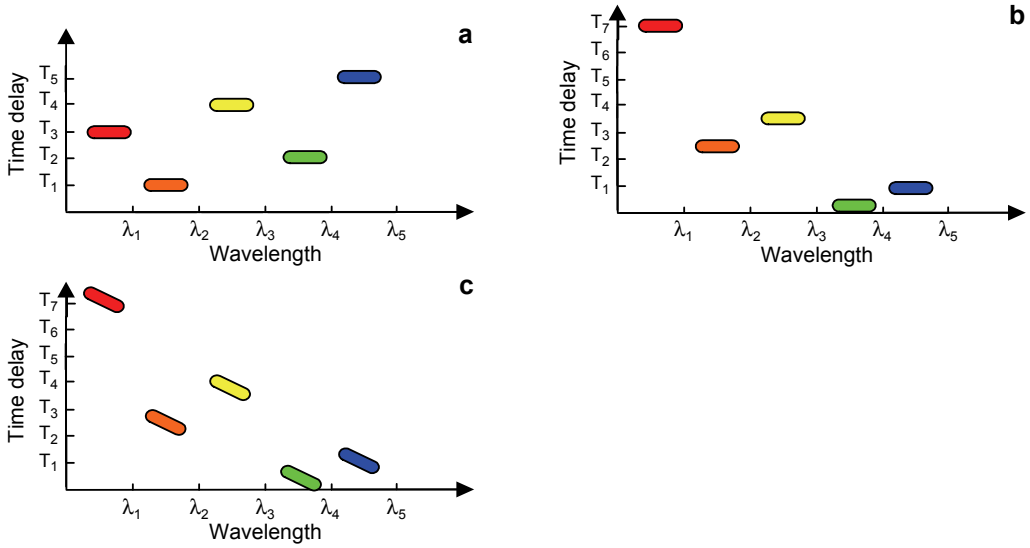


Fig. 2. The $\tau-\lambda$ distribution of three different kinds of decoders: decoder without dispersion compensating function (a), out-band dispersion compensating function (b), and total dispersion (both out-band and in-band) compensating decoder (c).

Expression (3) represents our concept of designing a total-dispersion-compensating decoder. Corresponding to Fig. 1, Fig. 2 shows the $\tau-\lambda$ distribution of three different kinds of decoders.

It would not be easy to fabricate such a total-dispersion-compensating decoder by the conventional FBG fabrication method. However, based on the equivalent chirp (EC) principle [9] that makes use of the -1st order reflective channel of sampled FBG (SFBG) by varying the sampling periods, it becomes easy to experimentally realize the proposed decoder.

The refractive index modulation of an SFBG can be expressed as

$$\delta n(z) = \overline{\delta n_{\text{eff}}}(z) \left\{ 1 + \frac{1}{2} v(z) S(z) \left[\exp\left(j \frac{2\pi z}{A} + j\phi(z)\right) + \text{c.c.} \right] \right\} \quad (4)$$

where $\overline{\delta n_{\text{eff}}}(z)$ is the average effective index (DC index), $v(z)$ is the fringe visibility that also acts as the apodization function, A is the grating period that is determined by the phase mask, $\phi(z)$ describes the spatially-varying phase, $S(z)$ describes the sampling function. For a uniform SFBG with the sampling period of P , $S(z)$ can be written as

$$S(z) = \sum_m F_m \exp\left(j \frac{2m\pi}{P} z\right), \quad m = 0, 1, \dots \quad (5)$$

where F_m is the Fourier coefficient. Hence, the refractive index modulation of the SFBG can be rewritten as

$$\begin{aligned}\delta n(z) &= \overline{\delta n_{\text{eff}}}(z) \left\{ 1 + \frac{1}{2} v(z) \sum_m F_m \left[\exp\left(j \frac{2m\pi}{P} z\right) \exp\left(j \frac{2\pi z}{A}\right) + \text{c.c} \right] \right\} = \\ &= \overline{\delta n_{\text{eff}}}(z) + \frac{1}{2} \sum_m \overline{\delta n_{\text{eff}}}(z) v(z) F_m \exp\left\{ j \frac{2\pi z}{(1/A + m/P)^{-1}} \right\} + \text{c.c} \quad (6)\end{aligned}$$

Equation (6) shows that the SFBG consists of a series of equivalent ghost gratings with the grating periods of $(1/A + m/P)^{-1}$. For the -1^{st} order ghost grating, the refractive index modulation can be written as

$$\delta n_{-1}(z) = \overline{\delta n_{\text{eff}}}(z) + \frac{1}{2} \overline{\delta n_{\text{eff}}}(z) v(z) F_{-1} \exp\left\{ j \frac{2\pi z}{(1/A - 1/P)^{-1}} \right\} + \text{c.c} \quad (7)$$

The grating period of the -1^{st} order ghost grating (producing the -1^{st} order reflective channel) can be expressed as:

$$A_{-1} = \frac{1}{\frac{1}{A} - \frac{1}{P}} = \frac{\Lambda P}{P - \Lambda} \quad (8)$$

Expression (8) shows that different -1^{st} order ghost gratings can be produced just by varying the sampling period based on a single uniform phase mask. Furthermore, only the sub-micrometer control-precision is required, since the sampling period is usually in the order of hundreds of microns.

For compensating the out-band dispersion, the spacing between SFBG's segments i (producing the -1^{st} order wavelength λ_i) and j (producing the -1^{st} order wavelength λ_j) is determined by the relative time delay between the two corresponding chips:

$$S = \frac{c}{2n_{\text{eff}}} \left(\Delta T_i^{\text{enc}} + \Delta T_i^{\text{out-disp}} - \Delta T_j^{\text{enc}} - \Delta T_j^{\text{out-disp}} \right) \quad (9)$$

For compensating the in-band dispersion, each SFBG's segment should chirp continuously. First, to achieve the bandwidth $\Delta\lambda$, the sampling periods of the two ends of the segment i should satisfy:

$$2n_{\text{eff}} |A_{-1,S} - A_{-1,E}| = 2n_{\text{eff}} \left| \frac{\Lambda P_S}{P_i - \Lambda} - \frac{\Lambda P_E}{P_i - \Lambda} \right| = \Delta\lambda \quad (10)$$

where $A_{-1,S}$ and $A_{-1,E}$ are the grating periods of the -1^{st} order ghost gratings in the starting and ending position of the segment i , respectively. P_S and P_E are the sampling periods in the starting and ending position, respectively. P_i is the average sam-

pling period that produces the -1 st order wavelength λ_i . The sampling period will increase or decrease gradually between the two ends.

Second, to achieve time delay $-\Delta T_{i, (\lambda - \lambda_i)}^{\text{in-disp}}$, the length L of the segment i should satisfy:

$$L = \left| \Delta T_{i, (\lambda - \lambda_i)}^{\text{in-disp}} \right| \frac{c}{2n_{\text{eff}}} \quad (11)$$

where c is the velocity of light in a vacuum. It should be noted that when the apodization of refractive index modulation is employed, a longer segment will be needed.

To conclude, expressions (9)–(11) are the basic principles of designing a total-dispersion-compensating decoder. These principles also apply to designing the total-dispersion-compensating encoder. For the sake of simplicity, the details will not be discussed.

3. Comparison and discussion

In the simulation, we use the prime-hop sequences (P0H1, P0H2, $p = 5$), the detailed parameters of coders are listed in Table 1.

Table 1. Parameters for total-dispersion-compensating en/decoders.

First central wavelength	Wavelength bin spacing	Bandwidth of bin	Time slot	Total dispersion	Length of each segment	Apodized profile of each segment
1550.4 nm	0.8 nm	0.24 nm	80 ps	360 ps/nm	17.2 mm	Gauss

The total dispersion, *i.e.*, 360 ps/nm, is equal to the dispersion of transmission in 20-km SMF. For comparison, the en/decoders without dispersion-compensating function and with out-band dispersion-compensating function are also simulated. Figure 3 shows their spectral properties.

To validate the decoding performance, the en/decoders data are loaded into a commercial simulation software. The simulation setup is shown in Fig. 4.

The broadband pulse sequence, loaded with user data, is sent into the encoders after a 5-nm bandwidth filter. The two encoders with different address codes are used to test the auto-correlation and cross-correlation properties simultaneously. The time-delay-line is used to de-correlate the two input data sources. There is no special dispersion-compensating module before the decoder after transmission in fiber ($D = 18$ ps/nm/km). The bandwidth of photodetector is 30 GHz. The repetition rate is set to be 10 Gbps and 40 Gbps, respectively.

The eye diagrams of decoded signals are shown in Figure 5. The results show that in the case of using normal en/decoder, the decoded pulse is rather broadened after 1.5 km transmission, and after 20 km transmission, the accumulated dispersion completely disorders the eye diagrams. In the case of using an out-band dispersion-compensating en/decoder, the residual in-band dispersion broadens the decoded pulse

to a bit duration after 20 km transmission at 10 Gbps, and further more, 20 km transmission at 40 Gbps makes the eye diagram completely closed. However, the total-dispersion-compensating en/decoder will largely reduce the influence of dispersion. In this case, the eye diagram after 20 km transmission at 10 Gbps is almost the same as that of back-to-back decoding with normal en/decoder. Either the encoder or

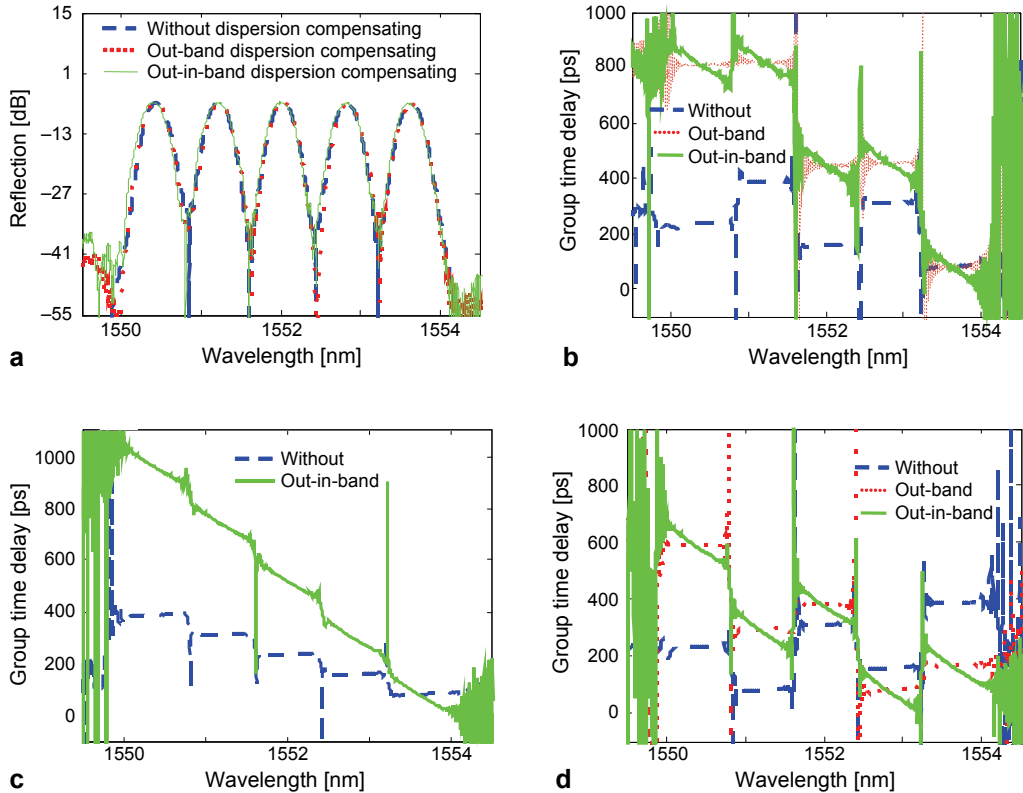


Fig. 3. Spectral properties of three kinds of en/decoders: amplitude spectrum of encoders with P0H2 (**a**); group time delay of encoders with P0H2 (**b**); group time delay of encoders with P0H1 (**c**); group time delay of decoders with P0H2 (**d**).

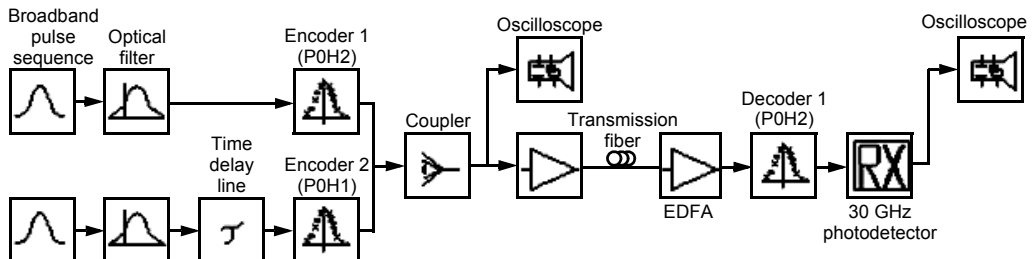


Fig. 4. Simulation setup.

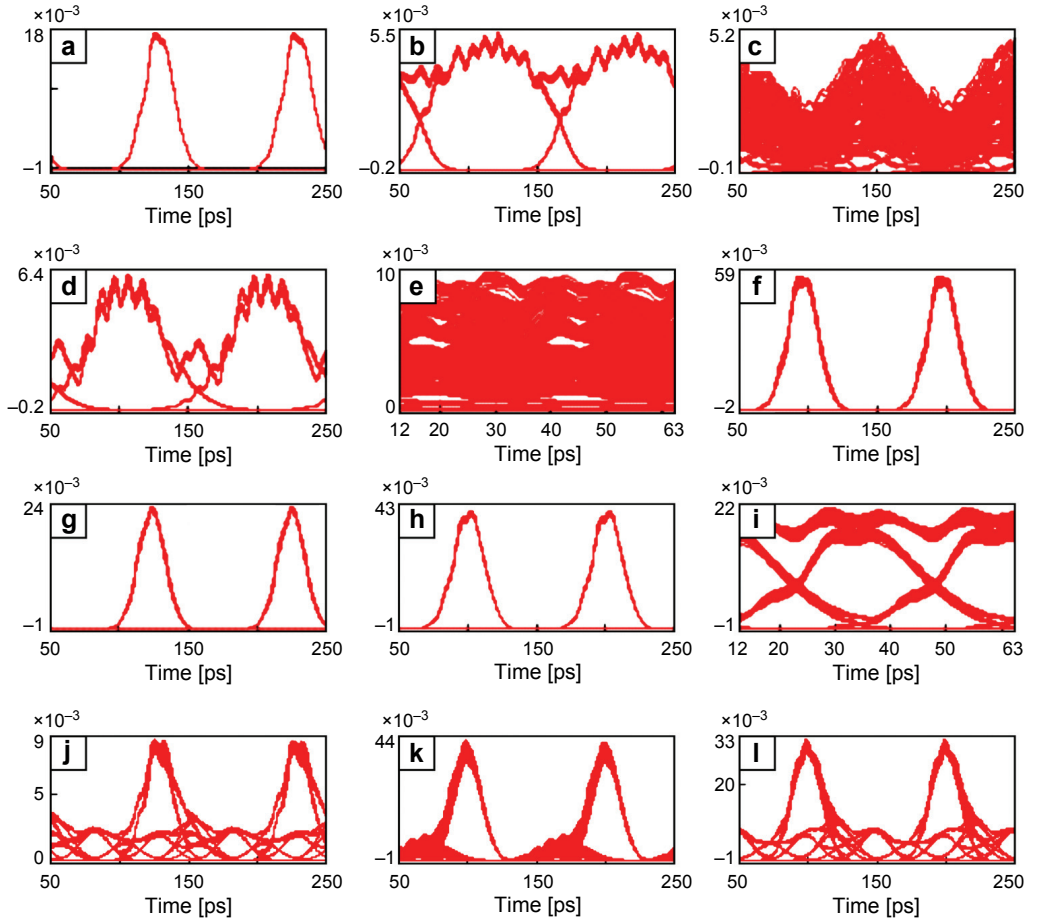


Fig. 5. Eye diagrams of decoded signals: are single-user results (a)–(i), are two-user results (j)–(l), specifically: back-to-back at 10 Gbps with normal en/decoder (a); 1.5-km transmission at 10 Gbps with normal en/decoder (b); 20-km transmission at 10 Gbps with normal en/decoder (c); 20-km transmission at 10 Gbps with out-band dispersion-compensating en/decoder (d); 20-km transmission at 40 Gbps with out-band dispersion-compensating en/decoder (e); 20-km transmission at 10 Gbps with total-dispersion-compensating en/decoder (f); 10-km transmission at 10 Gbps with total-dispersion-compensating encoder and normal decoder (g); 10-km transmission at 10 Gbps with normal encoder and total-dispersion-compensating decoder (h); 20-km transmission at 40 Gbps with total-dispersion-compensating en/decoder (i); back-to-back at 10 Gbps with 2 normal encoders and one normal decoder (j); 20-km transmission at 10 Gbps with 2 hybrid encoders (one is the normal encoder with P0H1 and the other is the total-dispersion-compensating encoder with P0H2) and one total-dispersion-compensating decoder with P0H2 (k); 20-km transmission at 10 Gbps with 2 total-dispersion-compensating encoders and one total-dispersion-compensating decoder with P0H2 (l).

the decoder is also verified to have the ability of compensating the dispersion of 10 km transmission, which is shown in Figs. 5g and 5h, respectively. Even in the case of 20 km transmission at 40 Gbps, a clear eye diagram can also be achieved by the total-dispersion-compensating en/decoder. The two-user results which are shown

as Figs. 5j–5l indicate that such total-dispersion-compensating en/decoders do not deteriorate the cross-correlation property.

4. Experimental validation

Based on the parameters in simulation, we experimentally fabricate the total-dispersion-compensating en/decoders. The fiber is hydrogen-loaded SMF, the pitch of a uniform phase mask is 1070 nm. The reflective spectrum and group time delay of en/decoders measured by optical vector analyzer (OVA) are shown in Fig. 6.

Due to the limitation of a broadband pulse source (not available in our laboratory), the system-scale experiment cannot be implemented. In order to test the fabricated en/decoder, the “measured data + simulation” method is used. The OVA-measured

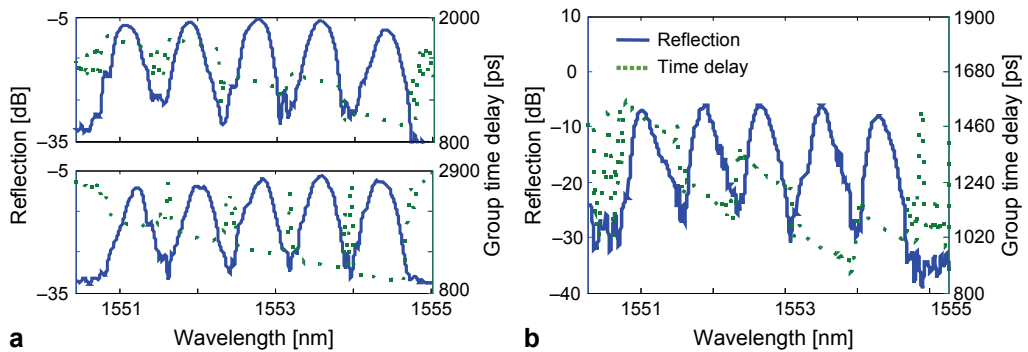


Fig. 6. Measured spectrum of total-dispersion-compensating coders: encoder, the upper part is with P0H2 and the lower P0H1 (**a**); decoder with P0H2 (**b**).

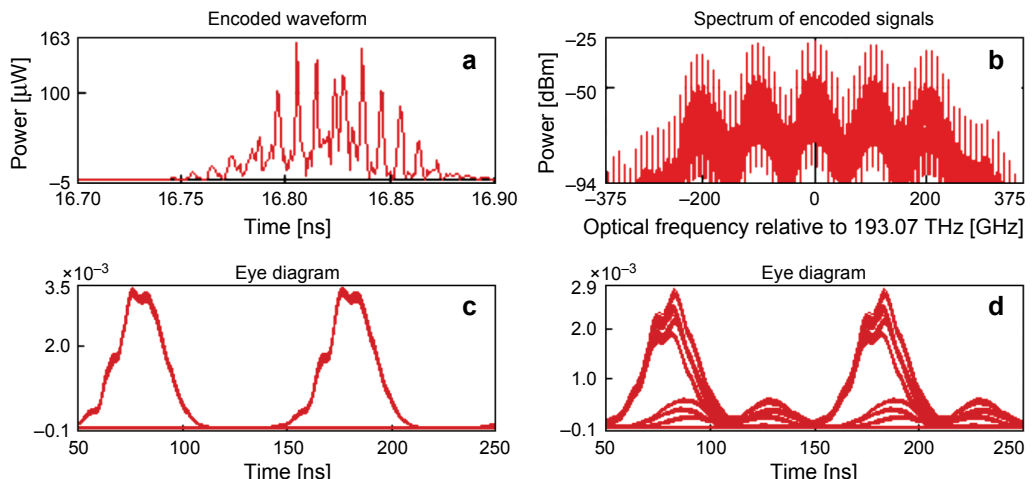


Fig. 7. Calculated results based on the measured spectra: encoded waveform for a single user (**a**); spectrum of encoded signals for a single user (**b**); eye diagram of decoded waveforms for a single-user after 20 km transmission (**c**); eye diagram of decoded waveforms for a two-user after 20 km transmission (**d**).

en/decoding spectra are loaded into the en/decoder modules in the commercial simulation software, as shown in Fig. 4. The encoded and decoded signals based on the measured data are calculated and shown in Fig. 7. It can be seen that although no special dispersion-compensating device is employed after 20 km transmission at 10 Gbps, the decoded pulse has not been broadened. The two-user result keeps good cross-correlation property. These results agree well with the simulation result. Therefore, the feasibility is verified that the fabricated en/decoder can compensate all the out-band and in-band dispersion induced by 20 km transmission in SMF.

5. Conclusions

In this paper, a novel total-dispersion-compensating en/decoder is proposed and investigated. Such en/decoders have two main advantages: *i*) the experimental fabrication can be realized only using a uniform-pitch phase mask and sub-micrometer precision moving stage, which brings low cost and high flexibility; *ii*) both the out-band and in-band dispersion can be compensated without any extra dispersion-compensating component. Such advances can make FBG-based en/decoders more powerful and make OCDM system more practical.

Acknowledgements – This work is partly supported by the Nature Science Foundation of Jiangsu Province under BK2012058 and the National Nature Science Foundation of China under 61032005, 60871075, 61174199 and 61177065. The authors would like to thank the anonymous reviewers for their careful reading and helpful comments.

References

- [1] KITAYAMA K., WADA N., SOTOBAYASHI H., *Architectural considerations for photonic IP router based upon optical code correlation*, Journal of Lightwave Technology **18**(12), 2000, pp. 1834–1844.
- [2] WADA N., SOTOBAYASHI H., KITAYAMA K., *Error-free transmission of 2-channel 2.5 Gbit/s time-spread/wavelength-hop OCDM using fiber Bragg grating with supercontinuum light source*, ECOC'99 Tech. Dig. II, 1999, pp. 230–231.
- [3] KITAYAMA K., *Code division multiplexing lightwave networks based upon optical code conversion*, IEEE Journal on Selected Areas in Communications **16**(7), 1998, pp. 1309–1319.
- [4] TANČEVSKI L., ANDONOVIC I., *Wavelength hopping/time spreading code division multiple access systems*, Electronics Letters **30**(17), 1994, pp. 1388–1390.
- [5] SCOTT R.P., CONG W., LI K., HERNANDEZ V.J., KOLNER B., HERITAGE J.P., YOO S.J.B., *Demonstration of an error-free 4×10 Gb/s multiuser SPECTS O-CDMA network testbed*, IEEE Photonics Technology Letters **16**(9), 2004, pp. 2186–2188.
- [6] ZHI JIANG, DONGSUN SEO, SHANGDA YANG, LEAIRD D.E., ROUSSEV R.V., LANGROCK C., FEJER M.M., WEINER A.M., *Four user 10 Gb/s spectrally phase-coded O-CDMA system operating at ~30 fJ/bit*, IEEE Photonics Technology Letters **17**(3), 2005, pp. 705–707.
- [7] TEH P.C., IBSEN M., LEE J.H., PETROPOULOS P., RICHARDSON D.J., *Demonstration of a four-channel WDM/OCDMA system using 255-chip 320-Gchip/s quarternary phase coding grating*, IEEE Photonics Technology Letters **14**(2), 2002, pp. 227–229.

- [8] TAMAI H., IWAMURA H., MINATO N., OSHIBA S., *Experimental study on time-spread/wavelength-hop optical code division multiplexing with group delay compensating en/decoder*, IEEE Photonics Technology Letters **16**(1), 2004, pp. 335–337.
- [9] CHEN XIANG-FEI, LUO YI, CHONG-CHENG FAN, TONG WU, SHI-ZHONG XIE, *Analytical expression of sampled Bragg gratings with chirp in the sampling period and its application in dispersion management design in a WDM system*, IEEE Photonics Technology Letters **12**(8), 2000, pp. 1013–1015.

*Received July 27, 2012
in revised form November 27, 2012*